

CARBON FIBERS

1. Introduction

Carbon fibers contain at least 90% carbon by weight obtained by pyrolysis of an appropriate precursor fiber (1). Graphite is one form of carbon. In graphite, the sp^2 hybridized carbon atoms are arranged in two-dimensional (2D) planes of hexagonal aromatic rings (1). These graphite planes are highly anisotropic due to the difference between in-plane and out-of-plane bonding of carbon atoms. The elastic modulus is much higher parallel to the plane than it is perpendicular to the plane. The bonding between graphite planes is van der Waals interaction, so the planes can slide with respect to one another. Carbon fibers are formed when long and thin graphite planes are packed together. Alignment of the graphite planes parallel to the fiber axis leads to high tensile modulus and electrical and thermal conductivity parallel to the fiber axis (2).

Polymeric materials that leave a carbon residue and do not melt upon pyrolysis in an inert atmosphere are generally considered candidates for carbon fiber production (3). The historical development of carbon fiber has been traced extensively (4). The first carbon fibers were produced by Edison in the United

States and Swan in England, respectively, from a cellulose precursor for light bulb filaments more than a century ago (5,6). Development of modern carbon fibers dates back to late 1950s and early 1960s by Watt in England (7), Shindo in Japan (8), and Bacon in the United States (9). Although cellulose was the early precursor used for carbon fibers, today polyacrylonitrile (PAN) is the predominant carbon fiber precursor, followed by petroleum pitch precursor. Carbon fibers are also being produced by decomposing gaseous hydrocarbons at high temperatures, and the first account of vapor grown carbon fiber (VGCF) production was in 1890 (10).

2. Processing of Carbon Fibers

2.1. PAN based Carbon Fibers. As mentioned, polyacrylonitrile is currently the predominant precursor for the carbon fibers due to a combination of tensile and compressive properties as well as to the carbon yield (11). PAN fibers were first developed by Dupont in the 1940s for use as textile fiber. Its thermal stability was recognized soon thereafter. This discovery led to further research on PAN fiber heat-treatment. In the early 1960s, PAN fibers were first carbonized and graphitized by Shindo (8) at the Government Industrial Research Institute, Osaka, Japan, and these fibers exhibited tensile strength and modulus of 0.75 GPa and 112 GPa, respectively. The process involved using tension in both the stabilization and the carbonization steps. According to Toray's company history, Shindo's patent was licensed to Toray in 1970 by the Japanese Ministry of International Trade and Industry (MITI) to produce PAN-based Torayca carbon fibers. During the 1960s, Watt and Johnson at Royal Aircraft Establishment in England (12) and Bacon and Hoses at Union Carbide in the United States (13) also developed a method for producing carbon fibers from PAN.

The steps involved for producing carbon fibers from PAN include polymerization of PAN, spinning of fibers, thermal stabilization, carbonization, and graphitization (Fig. 1). PAN copolymers containing 2–15% acrylic acid, methacrylic acid, methacrylate, and/or itaconic acid are generally used for carbonization. The use of comonomers affects molecular alignment and the stabilization conditions. Typical carbon yield from PAN-based precursors is 50–60%.

PAN fibers can be spun by wet, melt, dry, gel, and dry-jet wet-spinning, with wet spinning being the commonly used process (14). In the wet-spinning process, the polymer is directly extruded in the coagulation bath and the fiber is subsequently drawn at $\sim 100^{\circ}\text{C}$. Wet-spun PAN precursor fibers typically have a circular or dog-bone-shaped cross section depending on fiber coagulation conditions. Using specially shaped spinnerets and other cross-sectional shapes, such as "C," "T," and star, as well as trilobal shapes have also been processed to influence the microstructure and properties of the resulting carbon fibers. The cross-section shape of the ultimate carbon fiber resembles the shape of the precursor fiber.

The typical diameter of the PAN precursor fiber is about 15 μm , which ultimately results in a carbon fiber of about 7 μm in diameter. When processed under comparable conditions, tensile strength of the carbon increases with decreasing fiber diameter. Therefore, higher tensile strength carbon fibers can be produced

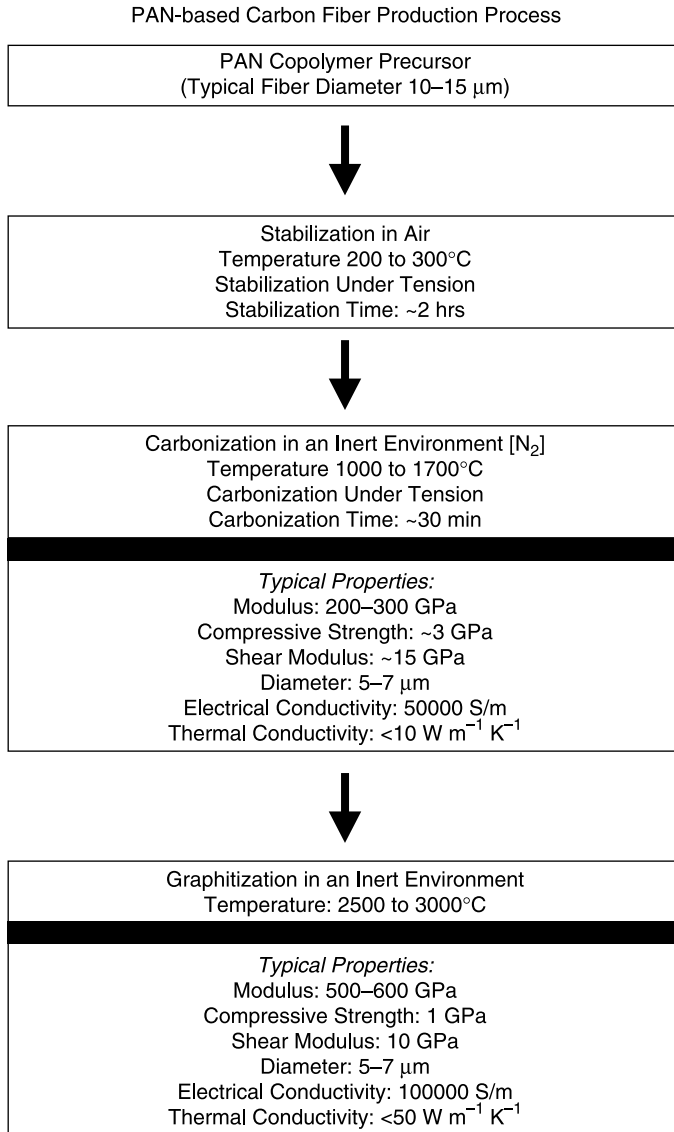


Fig. 1. PAN-based carbon fiber processing flow chart.

by decreasing the diameter of the PAN precursor fiber, and indeed, 5- μm -diameter carbon fibers with tensile strength of 7 GPa have been reported. However, the current fiber production technology makes it difficult and more expensive to process a PAN fiber with a diameter significantly below 15 μm . On the other hand, much smaller diameter PAN-based carbon fibers (100 nm to about 2 μm) can be processed by electrospinning. Carbonization of such small diameter PAN fibers has the potential to yield carbon fibers with tensile strength close to the theoretical value.

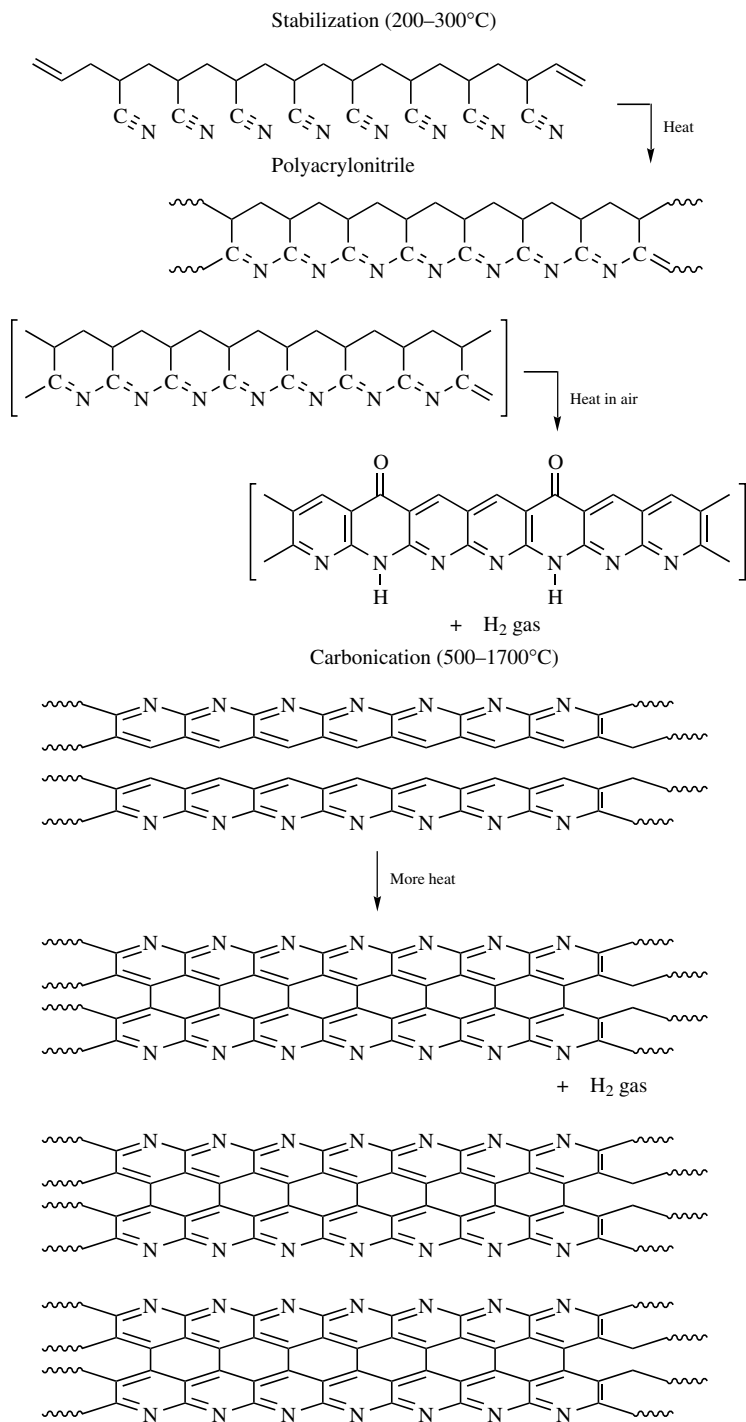


Fig. 2. Schematic representation of the carbon formation in PAN during stabilization and carbonization.

PAN fiber is stabilized under stress between 200°C and 300°C in an oxidizing atmosphere (15). During oxidative stabilization, PAN goes through chemical changes and results in increased density (16). During stabilization, PAN goes through cyclization and forms what is termed as the ladder polymer. During this step, some hydrogen evolution and oxygen pickup also occurs. A somewhat simplified version of what happens during stabilization is shown in Figure 2. As oxidative stabilization is a diffusion controlled process, the stabilization of the 15- μm -diameter PAN fiber generally takes about two hours, and stabilization time can vary with the copolymer composition. The stabilized fibers are carbonized in nitrogen in the 1000°C to 1700°C range. Various gases evolved during pyrolysis of PAN are shown in Figure 3 (17). Stretching during stabilization minimizes the need for stress during carbonization and graphitization. During the carbonization process, carbon content increases to above 90%, and the three-dimensional near-amorphous carbon structure with microcrystals form. These fibers can be further heat-treated between 2000°C and 3000°C (18) in an inert environment for graphitization. Nitrogen cannot be used in the graphitization process as it will react with the carbon to form nitrides. Modulus monotonically increases with heat-treatment temperature, whereas maximum strength is obtained at about 1500°C to 1600°C (Fig. 4) (19).

2.2. Pitch-based Carbon Fibers. Both isotropic and mesophase pitches are used to produce carbon fibers with low (100 GPa) and high moduli (up to 900 GPa), respectively. Pitch is produced from petroleum or coal tar that is made up of fused aromatic rings. Pitch-based carbon fibers are theoretically capable of modulus equal to graphite at 1050 GPa. This is significantly higher than the highest modulus obtained from PAN-based carbon fibers of 650 GPa (11). Pitch-based carbon fibers also demonstrate better electrical

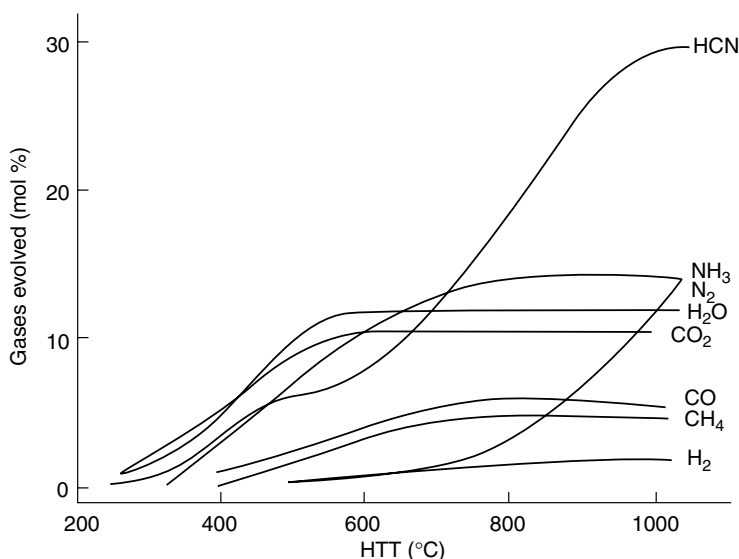


Fig. 3. Gases released during pyrolysis of PAN.

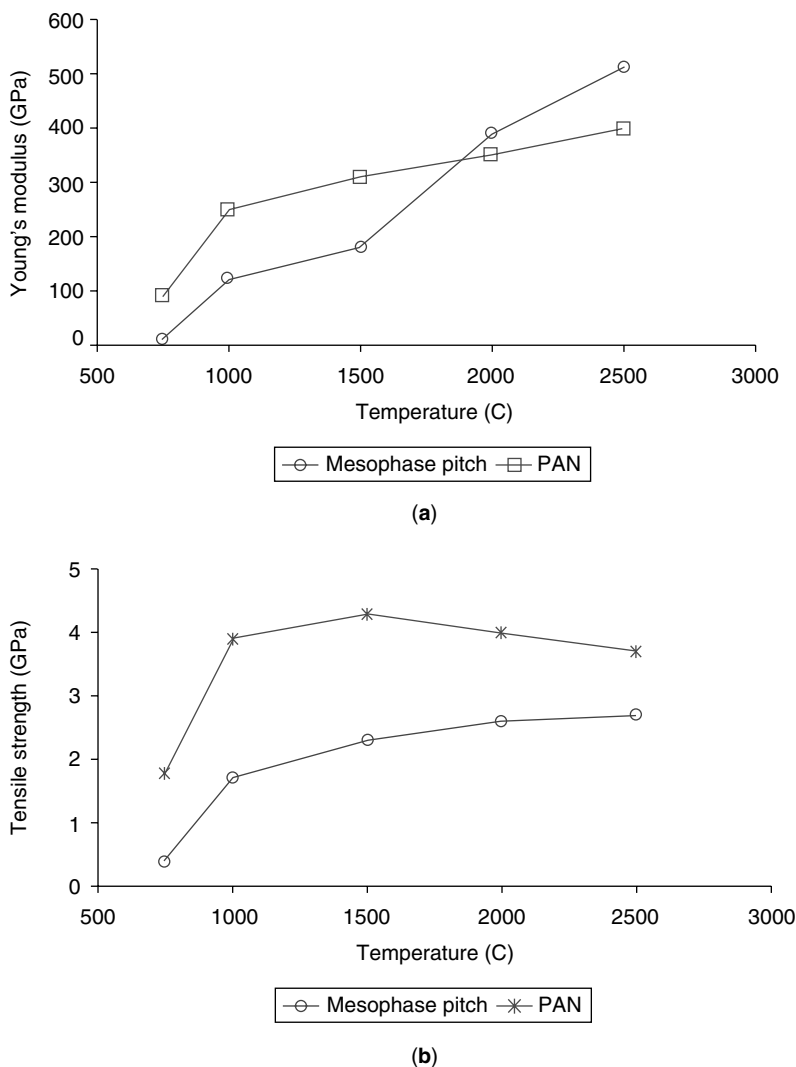


Fig. 4. (a) Young's modulus and (b) tensile strength as a function of heat treatment temperature for both PAN- and mesophase pitch-based carbon fibers.

and thermal properties than PAN-based fibers. Isotropic pitch-based carbon fibers were first commercialized in the 1960s, but mesophase pitch was not commercialized until the 1980s (20,21). Mesophase pitch-based carbon fiber production is an expensive process when compared with PAN-based carbon fiber production. Production of pitch-based carbon fibers involve melt spinning of pitch precursor fibers, stabilization (oxidation), carbonization, and graphitization.

The isotropic pitch has a softening point between 40°C and 120°C (22). The mesophase pitch is an anisotropic liquid crystal state of pitch consisting of disk-like aromatic molecules also known as carbonaceous pitch with a softening point around 300°C. This form of pitch is produced by pyrolysis of isotropic pitch

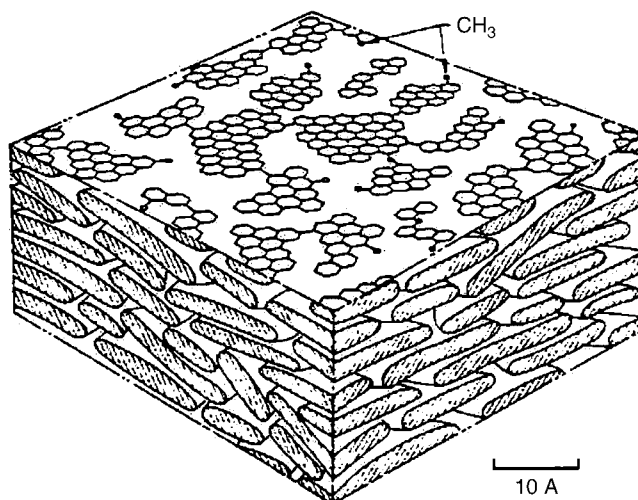


Fig. 5. Model of carbonaceous mesophase: a lamellar liquid crystal.

between 300°C and 500°C (23,24). A schematic diagram of the mesophase pitch is shown in Figure 5 (25). Before spinning, isotropic and mesophase pitches are purified using several methods. The molecular weight of pitch is typically in the 150–1000-g/mole range with an average molecular weight being about 450 g/mole. Pitch is melt spun into a continuous fiber, which can be drawn. The spinning temperature for mesophase pitch is around 350°C. The cross section of the spinneret hole not only controls the shape of the fiber but can also be used to control the microstructure of the final carbon fibers. The transverse microstructures of the pitch-based carbon fibers also changes with specific spinning conditions (Fig. 6) (26). The diameter of the pitch-based carbon fibers is typically about 10 μm .

Stabilization is a necessary step for pitch precursor fibers and takes place at temperatures between 200°C and 300°C. Pitch fibers will soften and melt at higher temperatures because it behaves like a thermoplastic. During stabilization, the thermoplastic is converted to a thermoset, and only then can it undergo high-temperature carbonization. The degree of stabilization is carefully controlled; otherwise, during carbonization, the fiber will melt if there is not sufficient stabilization. On the other hand, prolonged stabilization leads to a decrease in the final carbon fiber mechanical properties. The stabilization time for isotropic pitch is typically greater than that for the mesophase pitch. Pitch precursor fibers undergo carbonization and graphitization. The carbon yield for pitch-based fibers is highest of all precursors and is about 70–80%.

2.3. Cellulose-based Carbon Fibers. Man-made cellulosic fibers, such as Rayon, are used to produce carbon fibers. As mentioned, Edison (5) and Swan (6) first produced cellulose-based carbon fibers for light bulb filament application. The first commercial production of Rayon-based carbon fibers was carried out by Union Carbide in the 1960s. There are three main stages for Rayon-based carbon fibers: (1) low-temperature decomposition, (2) carbonization, and (3) graphitization. Rayon fibers are heated to 100°C in an inert atmosphere to remove water

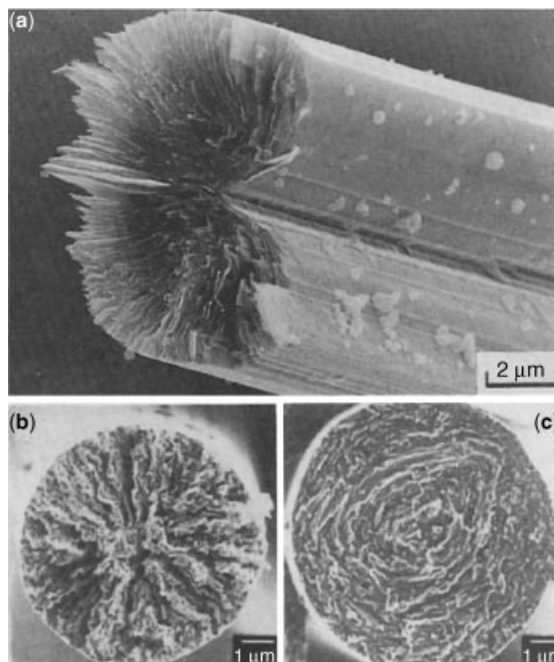


Fig. 6. Typical transverse microstructures for pitch-based carbon fibers showing (a) radial with wedge, (b) radial, and (c) concentric microstructure.

molecules. The temperature is gradually raised to 400°C; during which time, structural changes occur with a total weight loss of ~70%. The Rayon fibers are carbonized while stretching. The carbon yield for Rayon-based fibers range from 10% to 30% (15,24). The mechanical properties show improvement after graphitization with Young's modulus ranging from 170 to 500 GPa and tensile strength from 1 to 2 GPa for some commercial fibers. Rayon precursor is also used for making activated carbon fiber. The production of rayon-based carbon fibers is now almost nonexistent.

2.4. Gas-Phase Grown Carbon Fibers. Gas-phase grown carbon fibers are also known as vapor-grown carbon fibers (VGCFs). VGCFs are made by decomposing gaseous hydrocarbons at temperatures between 300°C and 2500°C in the presence of a metal catalyst like Fe or Ni that is either fixed to a substrate or fluidized in space (27). Typical substrates are carbon, silicon, and quartz, whereas hydrocarbons can be benzene, acetylene, or natural gas. Bahl et al. have traced the historical development of VGCFs (11). There are several reports on the development of VGCFs between 1890 and the 1980s (10,28–33); however, the development of VGCFs in general and vapor-grown carbon nanofibers in particular picked up steam during the 1990s, a result that at least in part can be attributed to the recognition and ensuing development of carbon nanotubes. An attempt was made to commercialize VGCF in the 1950s by Pittsburgh Coke and Chemical Company (30), but it was not successful. The properties of the carbon fibers are affected by the residence time of thermal decomposition and the temperature of the furnace. Growth mechanisms for

VGCF have been proposed by Baker et al. (34), Baired et al. (35), and Oberlin et al. (36). Diameters of VGCF range from 0.1 to 100 μm with circular, helical, and twisted cross sections (11,37). Vapor grown carbon nanofibers can now be obtained from Applied Sciences, Inc. (38) and Showa Denko (39).

2.5. Carbon Nanotubes. Carbon nanotubes (CNTs) were first reported by Iijima (40) in 1991 and since then have been the subject of intensive research due to their remarkable mechanical (41), electrical (42), and thermal (43) properties. CNTs can be classified into single wall nanotubes (SWNTs, typical diameter 0.7 to 1.5 nm), double wall nanotubes (DWNT, typical diameter, 2 to 5 nm), and multi-wall nanotubes (MWNT, typical diameter 5 to 50 nm). SWNT are composed of a single graphene layer rolled into a seamless cylinder. SWNTs can be semiconducting or metallic depending on the diameter and chiral angle (44) (0° to 30°) of the tube. DWNTs consist of two concentric tubes, whereas MWNTs are made of more than two concentric tubes. Nanotubes are synthesized by several methods, including arc discharge (45), catalytic chemical vapor deposition (CCVD), and the high-pressure carbon monoxide (HipCo) process (46).

SWNTs can be thought of as the ultimate carbon fiber because of their perfect graphitic structure, low density, and alignment with respect to each layer, giving them exceptional engineering properties and light weight. The elastic modulus parallel to the nanotubes axis is estimated to be ~ 640 GPa (47) and the tensile strength to be ~ 37 GPa (48). SWNT electrical and thermal conductivity at 300 K are 10^6 S/m (49) and ~ 3000 W/mK (50), respectively. The combination of density, mechanical, thermal, and electrical properties of SWNTs is unmatched, as there are no other materials with this combination of properties. The translation of these properties into macroscopic structures is the subject of current challenge for the material scientists and engineers.

3. Structure, Properties, and Morphology of Carbon Fibers

3.1. Structure and Morphology. The fine structure of carbon fibers consists of basic structural units of turbostratic carbon planes (Fig. 7a) (51). The distance between turbostratic planes is generally >0.34 nm, whereas the distance between perfect graphite planes is 0.3345 nm (Fig. 7b) (51). Carbon fibers typically exhibit a skin-core texture that has been confirmed using optical microscopy (52). The skin can result from higher preferred orientation and a higher density of material at the fiber surface (15). The formation of the skin is also associated with the coagulation conditions during PAN precursor fiber spinning. A schematic model of the basic structural units for carbon fibers based on various characterizations is given in Figure 8 (53).

Typical structural parameters for the selected pitch and PAN based carbon fibers are given in Table 1. The crystallite size in the high-modulus pitch-based fibers is as high as 25 nm along the c-axis direction and is 64 nm along the a-axis parallel to the fiber axis and 88 nm along the a-axis perpendicular to the fiber axis. Crystallite dimensions in fibers such as K-1100 are expected to be even larger. The crystallite size in the PAN-based carbon fibers (T-300 and IM-8) is in the 1.5- to 5-nm range. High-modulus pitch-based carbon fibers exhibit high orientation ($Z = 5.6$), whereas the orientation of the pitch-based carbon fibers is

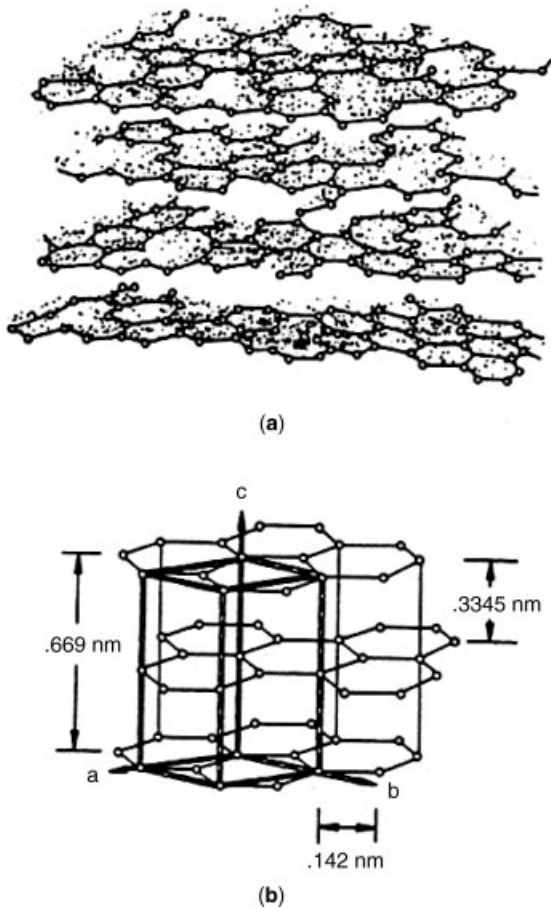


Fig. 7. (a) Turbostratic carbon and (b) structure of graphite and its unit cell.

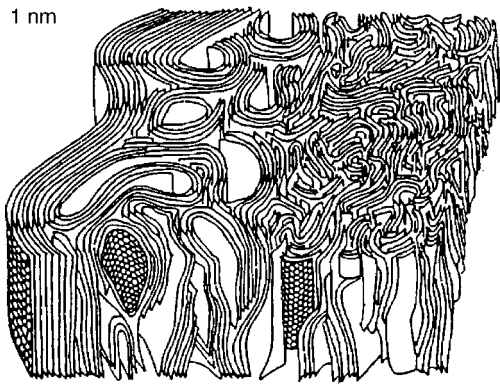


Fig. 8. Schematic of basic structural units arranged in a carbon fiber.

Table 1. Structural Parameters of Various Carbon Fibers

Fiber	L_c (nm)	L_a (0°) (nm)	L_a (90°) (nm)	Z (°)	$d_{(002)}$	3D Order	SEM Morphology
P-25	2.6	4	6	31.9	0.344	No	Sheet-like
P-55	12.4	11	30	14.1	0.342	Maybe	Sheet-like
P-100	22.7	49	80	5.6	0.3382	Yes	Sheet-like
P-120	25.1	64	88	5.6	0.3376	Yes	Sheet-like
T-300	1.5	2.2	4.1	35.1	0.342	No	No
IM-8	1.9	3.1	5.1		0.343	No	No

L_c = Crystal size parallel to c-axis.

L_a (0) = Crystal size parallel to a-axis and perpendicular to the fiber axis direction.

L_a (90) = Crystal size parallel to a-axis and parallel to the fiber axis direction.

z = Orientation parameter, full-width-at-half-maximum of the (002) azimuthal scan in degrees.

relatively low ($Z = 35.1$). High-modulus pitch-based carbon fibers (P-100 and P-120) also exhibit graphitic sheet-like morphology from scanning electron microscopy (Fig. 9a and b), as well as clear evidence of the three-dimensional order from X-ray diffraction (54). Due to the formation of microdomains, which can bend and twist, carbon fibers contain defects, vacancies, dislocations, grain boundaries, and impurities (20). Low interlayer spacing, large crystallite size, high degree of orientation parallel to the fiber axis, low density of defects, and high degree of crystallinity are characteristics of the high tensile modulus and high thermal and high electrical conductivity fibers. Porosity in carbon fibers are measured using SAXS (55), and this data can be used to estimate the size, shape, and orientation of the pores. Pore size, pore size distribution, and pore orientation changes as the fiber undergoes increasing heat-treatment and tension.

3.2. Properties. The tensile properties can be measured on single filaments or on a filament bundle (56,57). Fiber diameter can be measured using optical microscopy or laser diffraction (58). Properties of some commercial carbon fibers are listed in Table 2. As expected, carbon fiber properties are related to the fiber microstructure and morphology. Graphite elastic constants are listed in Table 3 (59). Orientation dependence of the graphite modulus is given by

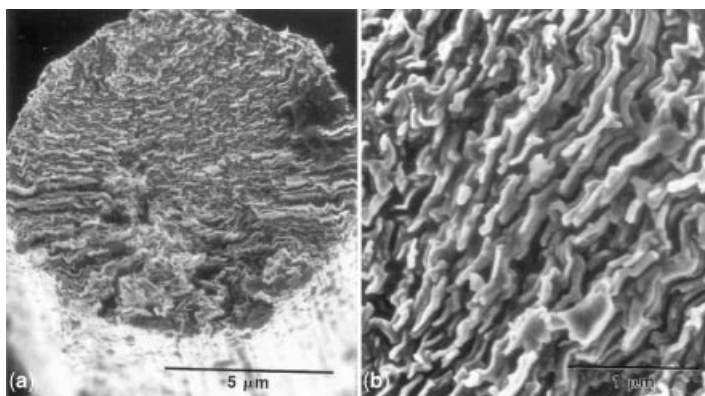



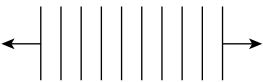
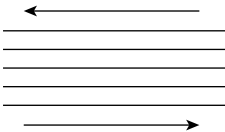
Fig. 9. SEM of pitch-based P-100 fiber at (a) low and (b) high magnification.

Table 2. Properties of Various High-Performance Fibers

Fiber	Tensile strength (GPa)	Tensile modulus (GPa)	Elongation to break (%)	Density, ρ (g/cm ³)	Thermal conductivity (W/mK)	Electrical conductivity (S/m)
Hexcel Magnamite® PAN-based						
AS4	4.27	228	1.87	1.79		6.54E + 04
AS4C	4.34	231	1.88	1.78		
IM4	4.79	276	1.74	1.78		
IM8	5.58	304	1.84	1.79		
PV42/850	5.76	292	1.97	1.79		
Cytec Thomel® PAN-based						
T300	3.75	231	1.4	1.76	8	5.56E + 04
T650/35	4.28	255	1.7	1.77	14	6.67E + 04
T300C	3.75	231	1.4	1.76	8	5.56E + 04
Toray Torayca® PAN-based						
T300	3.53	230	1.5	1.76		
T700SC	4.90	230	2.1	1.80		
M35JB	4.70	343	1.4	1.75		
M50JB	4.12	475	0.9	1.88		
M55J	4.02	540	0.8	1.91		
M30SC	5.49	294	1.9	1.73		
Cytec Thomel® Pitch-based						
P-25	1.38	159	0.9	1.90	22	7.69E + 04
P-55S	1.90	379	0.5	1.90	120	1.18E + 05
P-100S	2.41	758	0.3	2.16	520	4.00E + 05
P-120S	2.41	827	0.3	2.17	640	4.55E + 05
K-800X	2.34	896		2.20	900–1000	6.67E + 05 to 8.33E + 05
K-1100	3.10	965		2.20	900–1000	7.69E + 05 to 9.09E + 05

Source: Toray, Hexcel, Cytec.

Table 3. Elastic Constants for Single-Crystal Graphite

Crystal directions	Elastic constant (GPa)	
<div></div> <div>Tension parallel to the basal planes</div>	E_1	1060
<div></div> <div>Tension across the basal planes</div>	E_2	36.5
<div></div> <div>Shear between planes</div>	G_{12}	4

equation 1, and by using the elastic constants given in Table 3, modulus as a function of orientation has been plotted in Figure 10.

$$\frac{1}{\langle E \rangle} = \frac{1}{E_2} + \left[\frac{1}{G_{12}} - \frac{2\nu_{12}}{E_1} - \frac{2}{E_2} \right] \langle \cos^2 \theta_{\text{graphite}} \rangle + \left[\frac{1}{E_1} + \frac{1}{E_2} - \frac{1}{G_{12}} + \frac{2\nu_{12}}{E_1} \right] \langle \cos^4 \theta_{\text{graphite}} \rangle \tag{1}$$

where $\langle E \rangle$ is the tensile modulus, $\nu_{12} = 0.3$, and E_1 , E_2 , and G_{12} are found in Table 3.

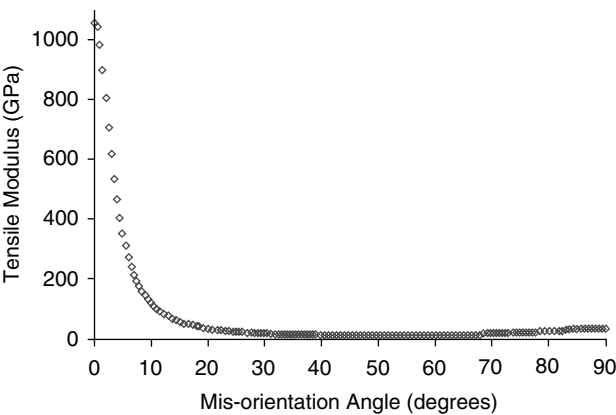


Fig. 10. Graphite tensile modulus versus misorientation angle.

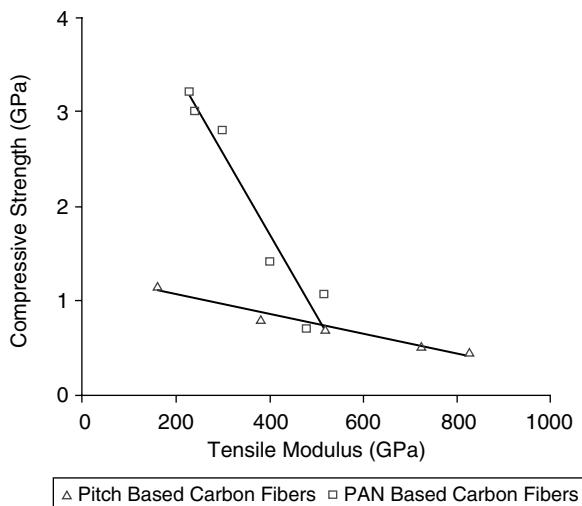


Fig. 11. Compressive strength versus tensile modulus for PAN- and pitch-based carbon fibers.

The axial compressive strength of PAN-based carbon fibers is higher than those of the pitch-based fibers (Fig. 11), and it decreases with increasing modulus in both cases. It is understood that higher orientation, higher graphitic order, and larger crystal size all contribute negatively to the compressive strength. PAN-based carbon fibers typically fail in the buckling mode, whereas pitch-based fibers fail by shearing mechanisms (Fig. 12) (60). This suggests that the compressive strength of intermediate modulus PAN-based carbon fibers may be higher than what is being realized in the composites. Changes in the fiber geometry, effective fiber aspect ratio, fiber/matrix interfacial strength, as well as matrix stiffness can result in fiber compressive strength increase, until the failure mode changes from buckling to shear. High compressive strength fibers also exhibit high shear modulus (Fig. 13) (54). Compressive strength dependence of pitch- and PAN-based carbon fibers on various structural parameters has been

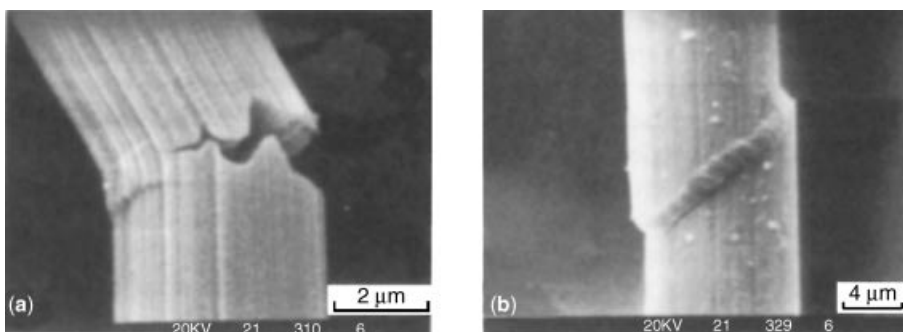


Fig. 12. (a) Kink bands in PAN-based carbon fiber after recoil compression under high deformation. (b) Shear bands in high-modulus mesophase pitch carbon fibers after moderate deformation.

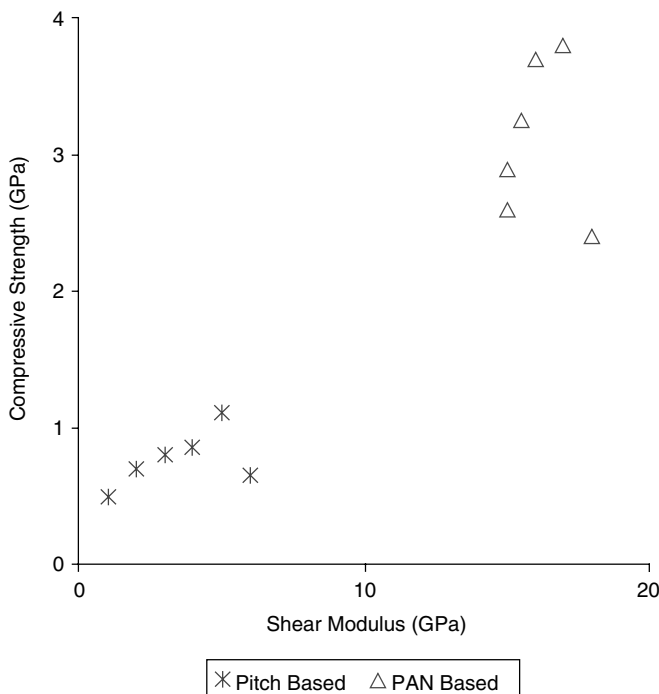


Fig. 13. Compressive strength versus shear modulus of various carbon fibers.

studied (54), and the compressive strength of high-performance fibers as well as compression test methods have been reviewed (61).

The electrical and thermal conductivities increase with increasing fiber tensile modulus and carbonization temperature (Fig. 14) (62,63). The electrical conductivity of PAN-based carbon fibers is in the range of 10^4 to 10^5 S/m, whereas that of the pitch-based carbon fibers is in the range of 10^5 to 10^6 S/m. The electrical conductivity increases with temperature because as the temperature is raised, the density and carrier (electrons and holes) mobility increases. Defects are known to cause carrier scattering. An increase in modulus is due to increased orientation of the carbon planes; this decreases the concentration of defects and subsequently decreases carrier scattering. The thermal conductivity of pitch-based carbon fibers is in the range of 20–1000 W/mK. Carbon fiber resistance to oxidation increases with the degree of graphitization. For carbon fibers, thermal gravimetric analysis in air shows the initial weight loss above 400°C, sharp weight loss in the 500–600°C range, and total weight loss by 850°C. Axial coefficient of thermal expansion of the 200- to 300-GPa modulus carbon fibers is in the range of -0.4 to $-0.8 \times 10^{-6}/^\circ\text{C}$, and for the high-modulus (700 to 900 GPa) carbon fibers, it is about $-1.6 \times 10^{-6}/^\circ\text{C}$.

4. Surface Treatment

The surface treatment (64) and surface properties of carbon fibers have been reviewed. Carbon fibers used in composite are often coated or surface treated

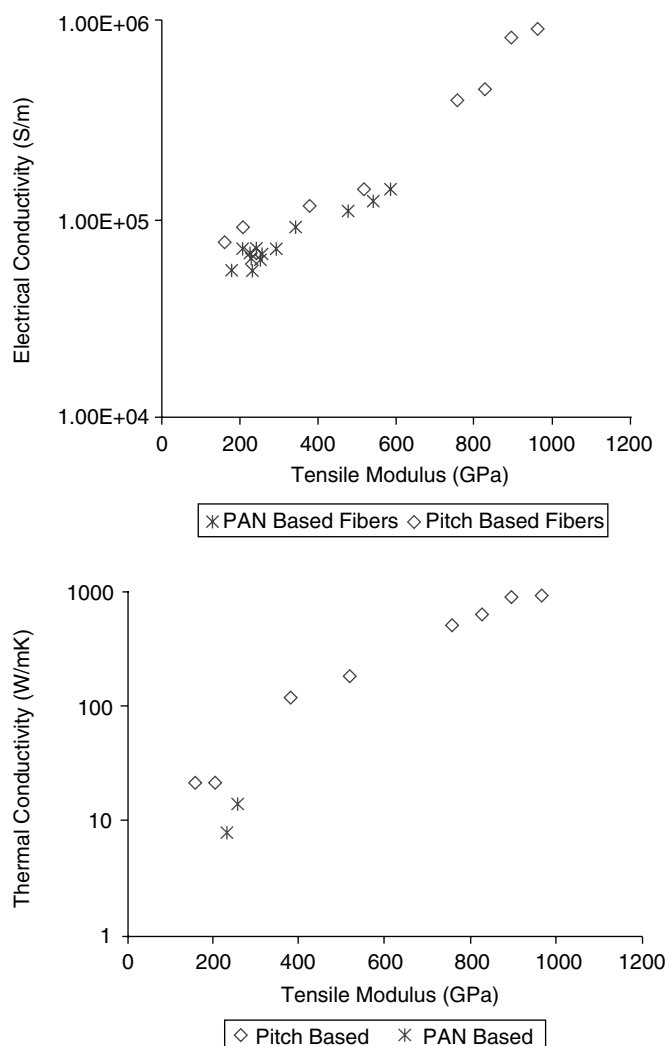


Fig. 14. (a) Electrical conductivity dependence on tensile modulus for both PAN-based and pitch-based carbon fibers. (b) Thermal conductivity dependence on tensile modulus for pitch- and PAN-based carbon fibers.

to improve interaction between the fiber surface and the matrix. Surface treatment usually results in development of specific polar groups and/or roughness on the surface for enhanced interaction with the matrix. Surface treatment can be oxidative (eg, in oxygen, nitric acid, or both oxidizing media) or nonoxidative. Nonoxidative treatment includes grafting of polymers or vapor phase deposition of pyrolytic carbon on the carbon fiber surface. Carbon fibers can be treated with plasma. Carbon fibers can be sized (application of thin coating) with epoxy resin or other polymers to make them compatible with a particular matrix. Interlaminar shear strength (ILSS) of surface-treated carbon fibers is reported to be in the range of 30–90 MPa, whereas the BET surface area for these surface-treated

carbon fibers is typically in the 25–60-m²/g range. As carbon fibers degrade in the presence of oxygen above 400°C and are stable in inert environment up to above 2000°C, they can be protected from oxidative degradation by application of a coating such as SiC, Si₃N₄, BN, and Al₂O₃.

5. Applications of Carbon Fibers

Worldwide production of carbon fibers has increased from 31 million pounds in 1997 to 41 million pounds in 2002, and it is projected to reach 56 million pounds by 2007 (65). The carbon fiber costs have come down significantly over the last 20 years, and the PAN- and pitch-based fiber production technology seems to have matured. Although intermediate-modulus carbon fibers can now be purchased for about \$10/lb and high-modulus highly conducting fibers can cost as high as \$1500/lb. Carbon fibers are used in aerospace, aircraft, nuclear, sporting goods, biomedical, and high-end automobiles. High strength, toughness, and low density of carbon fibers make them suitable for aerospace and sporting goods applications. Carbon fibers are also used for chemical protective clothing, electromagnetic shielding, and as fire-retardant nonwovens. Rayon-based carbon fibers are used for heat-shielding.

Carbon fiber composites are made with polymer, metal, ceramic, and carbon matrices. Although the composite materials do not yield the same mechanical properties as the fibers alone, the matrix adds other important properties to the composite for specific applications and holds the fiber together. As compared with most matrices, carbon fiber's coefficient of thermal expansion is typically two orders of magnitude lower; therefore, they can improve the dimensional stability of the composite. Although the early development of carbon fibers was prompted by defense and NASA applications, carbon fiber usage in the civilian aerospace industry is increasing at a rapid rate. For example, in the Boeing 767 model, carbon fiber composites made up 3% of the total materials (66); this increased to 7% for the latest Boeing 777 model, whereas the Boeing 787, to role off the assembly line in 2008, will consist of about 50 wt% composite materials and will use 20% less fuel than current airliners of the same size.

6. Quality Control and Specifications

Typically the quality control philosophy used for carbon fibers is based on a consistent precursor and tight control of processing parameters such as linespeed, temperature, and gas flow at each process step. Process control documents (PCDs) are used by some aerospace customers to assure consistent process conditions. Fiber physical and mechanical properties are tested statistically, along with some composites testing to assure the product meets specifications. Common fiber tests include yield (denier), density, strand strength, strand modulus, and size level. Composite tests include strength, modulus, and interlaminar shear strength (ILSS). Until recently, each carbon fiber producer established internal test procedures to assure product quality consistent with end-user requirements. In 1990, the Suppliers of Advanced Composite Materials

Association (SACMA) (organization no longer in existence; however, test methods are still used) established industry wide standards for carbon fiber test methods (67).

Most users require extensive composite qualification testing programs to assure acceptable end-use product properties. The magnitude of the qualification depends entirely on the end-use requirements and may range from extensive testing of laminates and final parts made from several production lots of fiber, to a single lot laminate evaluation or test coupon verification of properties.

7. Safety and Health Factors

Safety concerns in handling carbon fibers fall into three categories: dust inhalation, skin irritation, and electrical shorting of equipment. Additionally, the protective finish, or size, which is applied to the fiber may necessitate additional safety precautions. The most common sizes are epoxies that may contain cross-linking or curing agents that produce severe skin reactions. Groups such as SACMA provide general information on the safety of carbon fibers and composites. However, as carbon fiber sizes are specially formulated to match end-use requirements, it is best to consult with the Material Safety Data Sheet (MSDS) available from the suppliers for specific handling requirements.

7.1. Dust Inhalation. During processing, fine carbon filaments (5–10 μm in diameter) may break and be circulated in the air as a carbon dust that can be inhaled by operators. Studies (68–70) show that the fibers are too large to represent a respiratory health risk. Smaller diameter carbon fibers ($\sim 3.5 \mu\text{m}$) can enter the respiratory tract; however, there is no evidence of respiratory damage (71). They often create discomfort, and a protective mask is recommended when working in areas where carbon fiber dust is present.

7.2. Skin Irritation (72). Fine broken filaments often irritate the skin, occasionally causing transient itching and rashes. The back of hands and wrists and neck areas tend to be most sensitive. Protective clothing and barrier skin creams help prevent the fiber from reaching the skin and causing discomfort.

7.3. Electrical Hazards. Because carbon fibers are conductive, the airborne filaments can create serious problems shorting out electrical equipment. The best option is to locate sensitive equipment in clean rooms outside of areas where carbon fiber is being processed. If this is not possible, electrical cabinets must be effectively sealed to prevent contact with carbon fibers. A filtered air-positive purge provides additional protection for sensitive equipment.

8. Prospects

Carbon fiber modulus ($\sim 900 \text{ GPa}$) close to the theoretical value (1060 GPa) has been achieved. However, the experimental tensile strength achieved to date is only 10% to 20% of the theoretical estimates ($>30 \text{ GPa}$). If we look 100 years back, then the only available fibers were natural cellulosic fibers such as cotton, protein fibers such as wool and silk, as well as the man-made fiber, Rayon. The tensile strength of these fibers was less than 0.5 GPa. Today we have several

fibers with tensile strength ten times this value. Although carbon fiber processing from PAN and pitch seems to have matured, PAN/carbon nanotube composite fibers have been processed (73–75), exhibiting improved tensile modulus and strength and reduced thermal shrinkage when compared with the control PAN fibers. These PAN/nanotube composite fibers are good candidates for the development of next-generation carbon fibers with improved tensile strength and modulus while retaining compressive strength (76). Carbon fiber tensile strength increases with decreasing diameter. Therefore, it is expected that the small diameter PAN fibers (~100 nm) may exhibit significantly higher tensile strength values than achieved so far.

9. Acknowledgments

This article is adapted with permission from M. L. Minus and S. Kumar, “The Processing, Properties, and Structure of Carbon Fibers,” *JOM*, 2005, Vol. 57, No. 2, pp. 52–58.

BIBLIOGRAPHY

“Carbon (Baked and Graphitized Products, Uses)” in *ECT* 2nd ed., Vol. 4, pp. 202–243, by W. M. Gaylord, Union Carbide Corp.; “Carbon, Carbon and Artificial Graphite (Carbon Fibers and Fabrics)” in *ECT* 3rd ed., Vol. 4, pp. 622–628, by H. F. Volk, Union Carbide Corp.; “Carbon and Graphite Fibers” in *ECT* 4th ed., Vol. 5, pp. 1–19, by J. G. Venner, BASF Structural Materials, Inc.; “Carbon and Graphite Fibers” in *ECT* (online), posting date: December 4, 2000, by J. G. Venner, BASF Structural Materials, Inc.

CITED PUBLICATIONS

1. E. Fitzer, in J. L. Figueiredo, C. A. Bernardo, R. T. K. Baker, and K. J. Huttinger, eds., *Carbon Fibers Filaments and Composites*, Kluwer Academic, Dordrecht, 1990, pp. 3–4.
2. D. D. L. Chung, *Carbon Fiber Composites*, Butterworth-Heinemann, Boston, 1994, pp. 3–11.
3. W. Watt, in A. Kelly and Yu. N. Rabotnov, eds., *Handbook of Composites—Volume I*, Elsevier Science, Holland, 1985, pp. 327–387.
4. J. B. Donnet and R. C. Bansal, *Carbon Fibers*, 2nd ed., Marcel Dekker, New York, 1990.
5. U.S. Pat. 223,398 (1880), T. A. Edison.
6. Brit. Pat. 4933 (1880), J. W. Swan.
7. W. Watt and co-workers, *The Engineer (London)* **221**, 815 (1961).
8. Shindo, *J. Ceram. Assoc. Japan* **69**, C195 (1961).
9. R. Bacon and M. M. Tang, *Carbon* **2**, 211 (1964).
10. L. Schutzenberger, *C. R. Acad. Sic. (Paris)* **111**, 774–778 (1890).
11. O. P. Bahl, Z. Shen, J. Gerald Lavin, and Rodger A. Ross, in J. B. Donnet, T. K. Wang, S. Rebouillat, and J. C. M. Peng, eds., *Carbon Fibers*, Marcel Dekker, New York, 1998, pp. 1–84.

12. Brit. Pat. 1,110,791 (1965), W. Watt and W. Johnson.
13. R. Bacon and T. N. Hoses, in R. B. Sanymour and G. S. Kirshambaum, eds., *High Performance Polymers, Their origin and Development*, Elsevier, New York, 1986, p. 342.
14. V. B. Gupta and V. K. Kothari, eds., *Manufactured Fibre Technology*, Chapman & Hall, London, 1997.
15. L. H. Peebles, *Carbon Fiber – Formation, Structure, and Properties*, CRC Press, Boca Raton, 1995.
16. A. Takaku and J. Shimizu, *J. Appl. Polym. Sci.* **29**, 1319 (1984).
17. A. K. Fiedler, E. Fitzer, and F. Rozploch, *11th Biennial Conf. on Carbon* **261** (1973).
18. J. B. Donnet and O. P. Bahl, *Encycl. Phys. Sci. Technol.* **2**, 517 (1987).
19. T. Matsumoto, *Pure Appl. Chem.* **57**, 1553 (1988).
20. U.S. Pat. 4,032,430 (1980), S. Chwastiak.
21. S. Kumar, *Ind. J. Fibre Textile Res.* **16**, 52–64 (1991).
22. J. D. Brooks and G. H. Taylor, *Chemistry and Physics of Carbon*, Marcel Dekker, New York, 1968, pp. 243–268.
23. M. Z. Özel and K. D. Bartle, *Turk J. Chem.* **26**, 417–424 (2002).
24. M. S. Dresselhaus, G. Dresselhaus, K. Sugihara, I. L. Spain, and H. A. Goldberg, *Graphite Fibers and Filaments*, Springer-Verlag, Germany, 1988.
25. J. E. Zimmer and J. L. White, *Adv. Liq. Crysts.* **5**, 157 (1982).
26. M. Inagaki and co-workers, *Tanso* **147**, 57 (1991).
27. M. Endo, *CHEMTECT* **568** (1988).
28. J. Gibson et al., *Nature* **154**, 544 (1944).
29. T. Koyama, *Carbon* **10**, 757 (1972).
30. Anon., *Chem. Eng.* 172–174 (October, 1957).
31. U.S. Pat. 4,565,684 (1986), G. G. Tibbetts and M. G. Devour.
32. M. Endo, T. Koyama, and Y. Hishiyama, *Jpn. J. Appl. Phys.* **15**, 2073 (1976).
33. H. Katsuki et al., *Carbon* **19**, 148 (1981).
34. R. T. K. Baker, M. A. Barber, P. S. Herris, and F. S. Feetes, *J. J. Warte* **26**, 51 (1972).
35. T. Baired, J. R. Fryer, and B. Grant, *Carbon* **12**, 591 (1974).
36. A. Oberlin, M. Endo, and T. Koyama, *Carbon* **14**, 133 (1976).
37. M. Endo et al., *Carbon* **39**, 1287 (2001).
38. Applied Sciences, Inc., Available: <http://www.apsci.com/home.html>.
39. Showa Denko, Available: http://www.sdkc.com/fine_carbon.asp.
40. S. Iijima, *Nature* **354**, 56 (1991).
41. M. M. Treacy, T. W. Ebbesen, and J. M. Gibson, *Nature* **381**, 678 (1996).
42. R. E. Smalley et al., *Science* **273**, 483 (1996).
43. M. S. Dresselhaus and P. C. Eklund, *Adv. Phys.* **49**(6), 705 (2000).
44. M. S. Dresselhaus et al., *Carbon* **33**(7), 883 (1995).
45. S. Iijima and T. Ichihashi, *Nature* **363**, 603 (1993).
46. P. Nikolaev, M. J. Bronikowski, R. K. Bradley, F. Rohmund, D. T. Colbert, K. A. Smith, and R. E. Smalley, *Chem. Phys. Lett.* **313**, 91–97 (1999).
47. G. Gao et al., *Nanotechnology* **9**, 184 (1998).
48. D. A. Walters and co-workers, *Appl. Phys. Lett.* **74**, 3803 (1999).
49. S. Berber, Y.-K. Kwon, and D. Tomanek, *Phys. Rev. Lett.* **84** (2000).
50. P. Kim, L. Shi, A. Majumdar, and P. L. McEven, *Phys. Rev. Lett.* **87**, 215502 (2001).
51. W. P. Hoffman, W. C. Hurley, and P. M. Liu, *J. Mater. Res.* **6**, 1685 (1991).
52. D. J. Johnson, *Nature* **279**, 142 (1979).

53. S. C. Bennett and D. J. Johnson, *Proc. 5th Industrial Carbon and Graphite Conf.* **1**, 377 (1978).
54. S. Kumar, D. P. Anderson, and A. S. Crasto, *J. Mater. Sci.* **28**, 423 (1993).
55. H. Peterlik, P. Fratzl, and K. Kromp, *Carbon* **32**, 939 (1994).
56. ASTM Standard D 3379-75 (1989).
57. ASTM D 4018-4081.
58. C. T. Li and J. V. V. Tietz, *J. Mater. Sci.* **25**, 4694 (1990).
59. O. L. Blakslee et al., *J. Appl. Phys.* **41**, 3373 (1970).
60. M. G. Dobb, M. G., D. J. Johnson, and C. R. Park, *J. Mater. Sci.* **25**, 829 (1990).
61. V. V. Kozey, H. Jiang, V. R. Mehta, and S. Kumar, *J. Mater. Res.* **10**, 1044 (1995).
62. J.-P. Issi and B. Nysten, in J. B. Donnet, T. K. Wang, S. Rebouillat, and J. C. M. Peng, eds., *Carbon Fibers*, Marcel Dekker, New York, 1998, pp. 371–461.
63. Cytec Industries, <http://www.cytec.com>; Toray Global, <http://www.toray.com>; Hexcel Fibers, <http://www.hexcelfibers.com>; Grafil Inc., <http://www.grafil.com>; Zoltek Inc., <http://www.zoltek.com>; SGL Carbon Group, <http://www.sglcarbon.com>.
64. T. K. Wang, J. B. Donnet, S. Rebouillat, and J. C. M. Peng, in J. B. Donnet, T. K. Wang, S. Rebouillat, and J. C. M. Peng, eds., *Carbon Fibers*, Marcel Dekker, New York, 1998, pp. 231–309.
65. F. Hajduk, Carbon Fiber Overview presented to National Academy of Sciences.
66. Boeing, <http://www.boeing.com>.
67. J. J. Banisaukas, *35th Int. SAMPE Symp.* **35**, 1840 (1990).
68. P. E. Owen, J. R. Glaister, B. Ballantyne, and J. J. Clary, *J. Occup. Med.* **28**(5), 373–376 (1986).
69. H. D. Jones, T. R. Jones, and W. H. Lyle, *Ann. Occup. Hyg.* **26**(1–4), 861–868 (1982).
70. S. A. Thompson, *Appl. Ind. Hyg.* **12** (1989).
71. R. S. Waritz, B. Ballantyne, and J. S. Clary, *J. Appl. Tox.* **18**(3), 215–223 (1998).
72. Materials Safety Data Sheet for various commercially produced carbon fibers.
73. H. G. Chae, M. L. Minus, and S. Kumar, *Polymer* **47**, 3494–3504 (2006).
74. H. G. Chae, T. V. Sreekumar, T. Uchida, and S. Kumar, *Polymer* **46**, 10925–10935 (2005).
75. T. V. Sreekumar, T. Liu, B. G. Min, H. Guo, S. Kumar, R. H. Hauge, and R. E. Smalley, *Adv. Mater.* **16**, 58–61 (2004).
76. B. G. Min, T. V. Sreekumar, T. Uchida, and S. Kumar, *Carbon* **43**(3), 599–604 (2005).

MARILYN L. MINUS

SATISH KUMAR

The Georgia Institute of Technology